ANL/NSE-19/1

Reactivity Feedback Modeling in SAM

Nuclear Science and Engineering Division

About Argonne National Laboratory
Argonne is a U.S. Department of Energy laboratory managed by UChicago Argonne, LLC under contract DE-AC02-06CH11357. The Laboratory's main facility is outside Chicago, at 9700 South Cass Avenue, Argonne, Illinois 60439. For information about Argonne and its pioneering science and technology programs, see www.anl.gov.

ANL-NSE-19/1

Reactivity Feedback Modeling in SAM

prepared by
G. Hu, G. Zhang, and R. Hu
Nuclear Science and Engineering Division, Argonne National Laboratory

February 2019

EXECUTIVE SUMMARY

System Analysis Module (SAM) is being developed at Argonne National Laboratory as a modern system-level modeling and simulation tool for advanced non-light water reactor safety analyses. It utilizes the object-oriented application framework MOOSE to leverage the modern software environment and advanced numerical methods. The capabilities of SAM are being extended to enable the transient modeling, analysis, and design of various advanced nuclear reactor systems. This report presents the development of Point-Kinetics modeling and reactivity feedback mechanisms in SAM. It also presents a new capability for predicting the thermal expansion in various structural components by coupling SAM with an external thermomechanics module (Tensor Mechanics) from the MOOSE framework.

The analysis of the transient behavior of a nuclear reactor requires the coupled simulation of reactor kinetics and thermal-hydraulics of the reactor core, especially for those unprotected transients where the reactor scram system may not function properly. The point kinetics model has been widely used for reactor safety analysis due to its simplicity to capture the transient behavior of the reactor. Various reactivity feedback models have been developed and integrated with the Point-Kinetics module, including fuel axial expansion, core radial expansion, fuel Doppler, and coolant density reactivity. The reactivity feedback models in SAM are similar to the respective models used in SAS4A/SASSYS-1. This report first presents the brief theory of the Point-Kinetics module and reactivity feedback models. A number of verification tests have been performed where the code simulations are compared to the analytical model results.

The reactivity feedback due to the thermal deformation, such as the fuel axial expansion and core radial expansion, is important for SFR transient analysis. Simplified thermal expansion models for the fuel pin and reactor constrain system (e.g. grid plate) are developed and verified in SAM. Additionally, a coupling interface is developed to couple SAM with external thermomechanical analysis modules for more accurate predictions of the thermal expansion of different components during the transients. The current coupling interface has been tested with the Tensor Mechanics module from MOOSE.

These point kinetics and reactivity feedback modeling capabilities have also been demonstrated by simulating the early stage of the unprotected loss-of-flow (ULOF) accident in the Advanced Burner Test Reactor (ABTR). Both the stand-alone SAM and coupled SAM and Tensor Mechanics simulations are performed. It is confirmed that the major physics phenomena in the heat transport system of the ABTR reactor are captured by SAM, and the point kinetics model, reactivity feedback models, and the coupling schemes are working well as expected.

Table of Contents

LIST OF FIGURES

LIST OF TABLES

1 Introduction

Over the past few years, the rapidly rising interest in advanced nuclear reactor technology has led to an increased need for the developments and applications of advanced computational tools for modeling and simulation. System Analysis Module (SAM) is being developed at Argonne National Laboratory as a modern system-level modeling and simulation tool for advanced non-light water reactor safety analyses [1]. It utilizes the object-oriented application framework MOOSE [2] to leverage the modern software environment and advanced numerical methods [3]. The capabilities of SAM are being extended to enable the transient modeling, analysis, and design of various advanced nuclear reactor systems.

The analysis of the transient behavior of a nuclear reactor requires the coupled simulation of reactor kinetics and thermal-hydraulics of the reactor core, especially for those unprotected transients where the reactor scram system may not function properly. The point kinetics model has been widely used for reactor safety analysis due to its simplicity to capture the transient behavior of the reactor. This report summarizes the recent development of Point-Kinetics modeling and reactivity feedback mechanisms in SAM, including:

1. *Development and enhancement of the Point-Kinetics model*. A Point-Kinetics model has been developed in SAM to enable the analysis of transient behavior of the reactor core power. It needs to be enhanced with considering additional reactivity feedback models.
2. *Development of reactivity feedback models*. Four types of reactivity feedback models, including fuel axial expansion, core radial expansion, fuel Doppler, and coolant density reactivity feedback, are implemented in SAM. Simplified thermal expansion models are developed for the prediction of thermal expansion in various components, e.g. fuel pin and reactor constraint systems.
3. *Development of coupling interface between SAM and external thermomechanical analysis module*. The capability of coupling SAM and external thermomechanical analysis module provides the option to predict the thermal deformation more accurately than the internal models in SAM. This coupling interface will also be useful in the future for coupling with other external modules.

A number of verification tests have been performed where the code simulations are compared to the analytical model results. Additionally, the full point kinetics and reactivity feedback modeling capabilities have also been demonstrated by simulating the early stage of the unprotected loss-of-flow (ULOF) accident in the Advanced Burner Test Reactor (ABTR). Both the stand-alone SAM and coupled SAM and Tensor Mechanics simulations are performed.

2 Point-Kinetics Model and Reactivity Feedback Mechanisms

2.1 Point-Kinetics Model

The analysis of the transient behavior of a nuclear reactor requires the coupled simulation reactor kinetics and thermal-hydraulics of the reactor core. The point kinetics model is widely used for the coupled simulation due to its simplicity to capture the transient behavior of the reactor. In the point kinetics model, it is assumed that the reactor power can be separated into space and time function. The assumption is adequate when the space distribution remains nearly constant during the transient. The Point-Kinetics model shown in Equation *(2-1)* and *(2-2)* has been widely used for the transient safety analysis of stationary fuel reactors [5].

$$\frac{dn}{dt} = \frac{\rho_{ext} - \tilde{\beta}_{eff}}{\Lambda} n + \sum_i \lambda_i C_i \qquad (2\text{-}1)$$

$$\frac{dC_i}{dt} = \frac{\beta_i}{\Lambda} n(t) - \lambda_i C_i \qquad (2\text{-}2)$$

where $n(t)$ is the total neutron population, normalized by the neutron population at full fission power; C_i is the magnitude of delayed-neutron precursor population i, normalized by the neutron population at full fission power; $\tilde{\beta}_{\text{eff}}$ is the total effective delayed-neutron fraction while β_i is the fraction for delayed neutron precursor i; ρ_{ext} is a fraction representing the net reactivity feedback; Λ is the prompt neutron generation time (t). The normalized fission power and delayed-neutron precursor population are solved simultaneously

The basic point-kinetics module has validated against forward Euler method and the calculation by SAS4A/SASSYS-1 [4]. The external reactivity is defined in Equation *(2-3)*, and the kinetic parameters used in the Point-Kinetics model are given in Table 2-1. The comparisons of the normalized fission power are shown in Figure 2-1 and excellent agreement is observed between the two code results.

$$\rho_{ext} = \begin{cases} 2t \text{ pcm } (0s < t < 2s) \\ -4t + 12 \text{ pcm } (2s < t < 7s) \\ 2t - 30 \text{ pcm } (7s < t < 8s) \\ -14 \text{ pcm } (8s < t) \end{cases} \qquad (2\text{-}3)$$

Table 2-1. Kinetics Parameters for the Benchmark Case

Parameters	Value
Decay constant (sec^{-1}), λ	
- group 1	0.01335
- group 2	2.87380
Effective DNP group fraction, β	
- group 1	0.0239%
- group 2	0.0492%
- total	0.0731%
Prompt neutron lifetime (sec), Λ	3.46402E-07

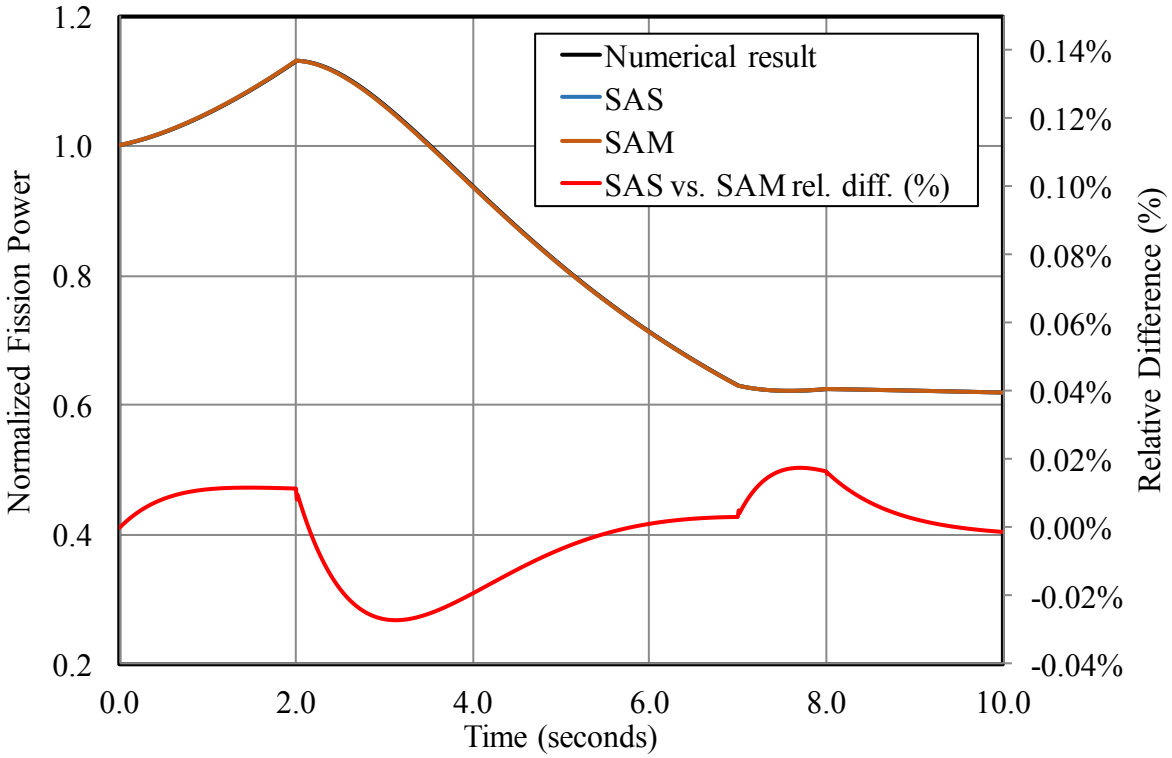

Figure 2-1. Comparisons of SAS4A/SASSYS-1 and SAM Normalized Fission Power along with Numerical Results

Four types of reactivity feedback have been developed for the transient simulations, including fuel axial expansion, core radial expansion, fuel Doppler, and coolant density reactivity feedback. The reactivity models in SAM are similar to the respective models used in SAS4A/SASSYS-1[4].

2.2 Fuel Axial Expansion Reactivity Feedback

2.2.1 Fuel Axial Expansion Reactivity Feedback

In advanced nuclear reactors (e.g. Sodium-cooled Fast Reactor), the fuel, especially metallic fuel, expands or shrinks within the cladding in response to the fuel temperature changes during the transient. The geometry changes of the fuel reactor impose a positive or negative reactivity feedback, which affects the prompt fission power calculation in the Point-Kinetics model.

The fuel axial expansion model is developed to consider the reactivity feedback in response to the fuel temperature changes during the transient. The fuel reactivity is integrated over the core channels (Equation *(2-4)*), and the difference between the transient and initial values (Equation *(2-5)*) is provided to the Point-Kinetics model for the calculation of fission power [4].

$$R_{\mathrm{A}}(t) = \int_{z=0}^{z=L} \rho_f(z,t) \times r_f(z) \times A \, dz \qquad (2\text{-}4)$$

$$\Delta R_{\mathrm{A}}(t) = R_{\mathrm{A}}(t) - R_{\mathrm{A}}^{ss} \qquad (2\text{-}5)$$

where R_A is the axial expansion feedback in the unit of Δk/k; $\rho_f(z,t)$ is the fuel density at transient time t in the unit of kg/m^3; $r_f(z)$ is the fuel reactivity coefficient in unit of $\Delta k/k/kg$; L and A are the fuel length and cross-section area, respectively. The integration will consider the transient axial displacements in the fuel pin, which will be provided by either coupled thermomechanical analyses or SAM standalone calculations. The coupling scheme will be discussed in Section 3.2. In case the coupled displacements are not provided, the following thermal expansion model is initialized to calculate the displacements, i.e. Equation (2-10) or Equation (2-12) depending on if the eutectic bonding is formed.

2.2.2 Axial Thermal Expansion Model for Fuel Pin

During the transient and steady-state simulations, the axial expansion in the fuel pellet (or fuel rod) is the variable of interest in modeling the reactivity feedback. There are two different situations depending on if the fuel pellet is in eutectic condition with the cladding:

- Case 1: Fuel pellet is in free expansion
- Case 2: Fuel pellet and the cladding are in eutectic condition

In Case 1, the cladding can be ignored in the thermal modeling, because the expansion in cladding will contribute little to the reactivity feedback. In Case 2, the gap will be ignored, the fuel rod will be constrained by the cladding in the radial direction. It is assumed that the fuel rod and cladding will expands freely but bound together in the axial direction. The schematic for modeling the axial expansion for these two cases is shown in Figure 2-2.

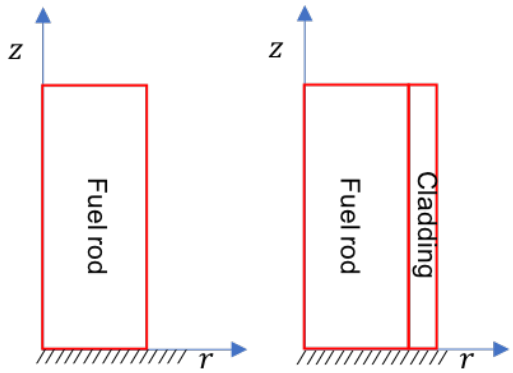

Figure 2-2. Schematic for modeling expansion in fuel rod in two conditions: free expansion (left) and eutectic condition (right)

For the thermal expansion model in the fuel pin, the gap and plenum pressure will be ignored, which gives the assumption of zero axial load. Due to the assumption of zero axial load, the integration of axial stress σ_{zz} over the radial cross section should vanish, i.e.,

$$F_z = \int_A \sigma_{zz} dA = 0 \qquad (2\text{-}6)$$

The problem of axially unrestrained plane strain deformation, such that the axial force is zero and the axial strain is constant, is called the general plane strain problem [7]. Let $\theta = T - T_{\text{ref}}$, where T_{ref} is the stress-free reference temperature. From Hooke's law, the stress-strain relation along the z-axis is

$$\varepsilon_{zz} = \frac{1}{E}\left[\sigma_{zz} - \nu\left(\sigma_{xx} + \sigma_{yy}\right)\right] + \alpha\theta \tag{2-7}$$

Integrating Equation (2-7) over the cross section, with the consideration of Equation (2-6), yields

$$E\bar{\varepsilon}_{zz} = -\nu\left(\bar{\sigma}_{xx} + \bar{\sigma}_{yy}\right) + E\alpha\bar{\theta} \tag{2-8}$$

where $\bar{\sigma}_{xx}$, $\bar{\sigma}_{yy}$, and $\bar{\theta}$ are the average over the cross section. When the external mechanical loads are zero in the cross section, $\bar{\sigma}_{xx} + \bar{\sigma}_{yy} = 0$, and Equation (2-8) results in

$$E\bar{\varepsilon}_{zz} = E\alpha\bar{\theta} \tag{2-9}$$

Equation (2-9) indicates that the axial displacement could be approximated with the average temperature in the cross section. Let $\bar{T}(z)$ being the axial temperature profile after averaging over the cross section. The axial displacement $w(z)$ will be approximated with

$$w(z) = \int_0^z \bar{\varepsilon}_{zz} dz = \int_0^z \alpha\bar{\theta}\, dz \tag{2-10}$$

When the fuel pellet and the cladding are in eutectic condition, there will be a strong shear stress in the fuel-cladding boundary. Let F_{rz} be the effective shear force in the boundary, w_1 be the free axial expansion in fuel rod, w_2 be the free axial expansion in the cladding, and w_e be the effective axial expansion after considering the eutectic condition. These variables are related by

$$w_e = w_1 - \frac{F_{rz}}{A_1}\frac{L}{E_1} = w_2 + \frac{F_{rz}}{A_2}\frac{L}{E_2} \tag{2-11}$$

where A_1 and A_2 are the cross-section area of fuel rod and cladding. Solving for F_{rz} from Equation (2-11), and then substitute the result into Equation (2-11), the effective axial expansion is

$$w_e = w_1\gamma_1 + w_2\gamma_2 \tag{2-12}$$

where

$$\gamma_1 = \frac{A_1E_1}{A_1E_1 + A_2E_2}, \qquad \gamma_2 = \frac{A_2E_2}{A_1E_1 + A_2E_2} \tag{2-13}$$

which indicates that the effective axial expansion in fuel pin is affected by the area and Young's modulus of fuel rod and cladding.

2.3 Core Radial Expansion Feedback Reactivity

2.3.1 Core Radial Expansion Reactivity Feedback

Due to temperature changes in the cooling system, the reactor core experiences radial thermal expansion, which impose a positive or negative reactivity feedback. For most advanced nuclear reactor design, there are also some constraint systems (e.g. Grid Plate, Above Core Load Pad, Top Load Pad), and the geometry of the reactor core during the transient is also affected by those constraint system (Figure 2-3).

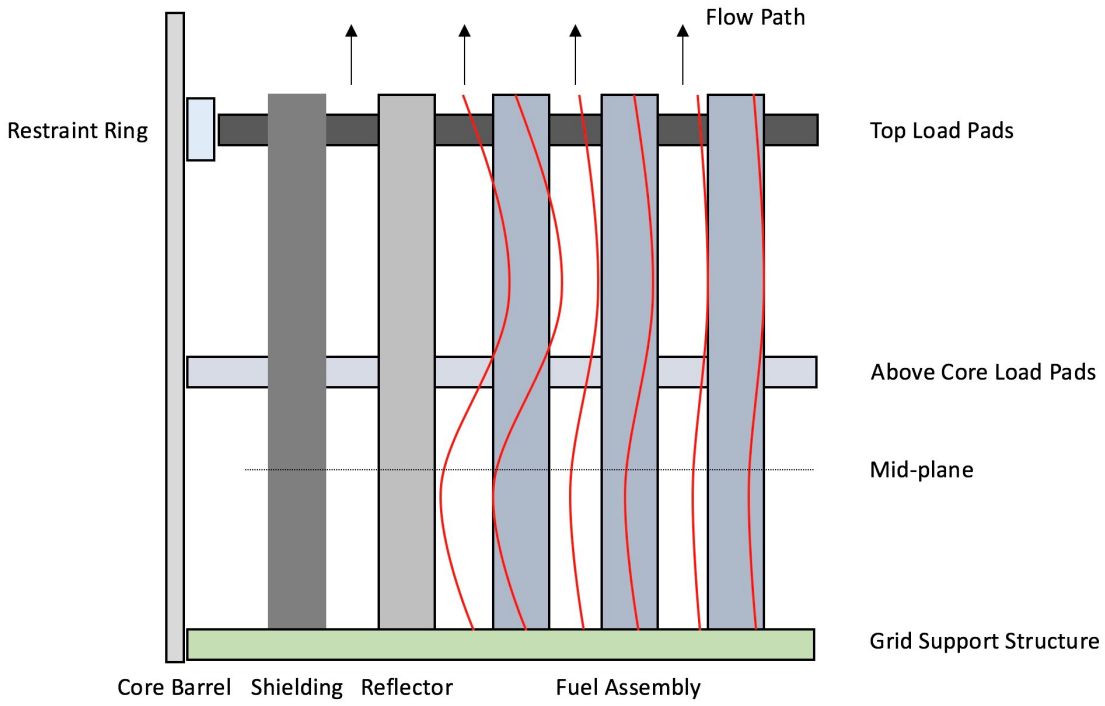

Figure 2-3. Restraint Systems in Typical SFR and Core Radial Expansion

The core radial expansion model is developed to consider the reactivity feedbacks in response to the thermal expansions of reactor cores during the transient. The current model implemented in SAM is able to consider the expansion effects based on multiple constraint systems (Figure 2-3). The reactivity feedbacks due to the expansion effects at different elevations are weighted by user-defined factors [4].

$$\Delta R_{RC}(t) = \sum_{n}^{N} \left(\frac{\Delta R}{R}\right)_n \times w_n \times \rho_{RC,n} \qquad (2\text{-}14)$$

where ΔR_{RC} is the core radial expansion feedback in the unit of $\Delta k/k$; $\Delta R/R$ is the relative change in the radius of reactor core; ρ_{RC}^{n} is core radial expansion coefficient at position n in the unit of $\Delta k/k$ *per* $\Delta R/R$; w_n is the user-defined weighting factor; N is the total number of the constraint systems. The displacement of individual constraint system is provided by either an external thermomechanical calculation or SAM standalone calculation. In case the displacement of individual constraint system is not provided by external calculations, the following thermal expansion model will be initialized to calculate the displacement of individual constraint system.

2.3.2 Core Radial Expansion Model

The core inlet grid plate or core load pads compose a core constraint system that is responsible for the radial expansion of the reactor core. For simplicity, the individual grid plate is assumed at uniform temperature that is equal to the coolant temperature at the elevation of corresponding constraint system. The geometry for the realistic grid plate is rather complicated (e.g. Figure 3-8,

right) for the thermomechanical analysis. In the current model, the grid plate would be simplified as a thin hollow disk to get an approximate estimate of core radial expansion.

Consider a thin hollow disk with an inside radius R_1 and an outside radius R_2 with a radial temperature profile $\theta(r) = T(r) - T_{\text{ref}}$. Assuming a plane stress condition [7], the general solution for a hollow disk is

$$u = (1+\nu)\frac{\alpha}{r}\int_{R_1}^{r}\theta r dr + C_1 r + \frac{C_2}{r} \tag{2-15}$$

where the integration constants, C_1 and C_2, are

$$C_1 = \frac{1-\nu}{2}\alpha\bar{\theta}, \qquad C_2 = \frac{1+\nu}{2}\alpha\bar{\theta}R_1^2 \tag{2-16}$$

where

$$\bar{\theta} = \frac{2}{R_2^2 - R_1^2}\int_{R_1}^{R_2}\theta r dr \tag{2-17}$$

If the temperature is uniform in the hollow disk (i.e. $\theta = \text{const}$), then

$$u = \alpha\theta r \tag{2-18}$$

which indicates that the radial displacement is linear with r. In this case, the displacement field in the grid plate could be approximated with Equation (2-18). The validity of the model will be confirmed in a verification test presented in Section 3.4.

2.4 Fuel Doppler Reactivity Feedback Model

The fuel Doppler reactivity model is implemented in SAM to consider the reactivity feedbacks in response to the fuel temperature changes during the transient. The Doppler reactivity feedback is integrated over the core channels (Equation (2-19)) and provided to the Point-Kinetics model for the calculation of fission power.

$$R_D(t) = \sum_{n}^{N} \alpha_D^n \times ln\left[T_f^n(t) \,/\, T_f^n(0)\right] \tag{2-19}$$

where R_{D} is the fuel Doppler reactivity feedback in the unit of Δk/k; α_D^n is the fuel Doppler reactivity coefficient of node n in unit of Δk/k per ln((T+ΔT)/T); $T_f^n(t)$ and $T_f^n(0)$ are the fuel temperature of node n at the time of t and the beginning, respectively; N is the total number of the nodes. The Doppler reactivity coefficient is generated from the neutronics calculations by perturbing the corresponding axial nodes in all the assemblies in a single core. All the assembly nodes on the same axial level are lumped together. The Doppler reactivity coefficients are provided as user inputs in SAM simulations. With user-provided fuel Doppler reactivity coefficients, the fuel temperature changes during the transient impose a positive or negative reactivity feedback on the fission power.

2.5 Coolant Density Reactivity Feedback

The coolant density reactivity model is developed to consider the reactivity feedbacks in response to the coolant temperature changes during the transient. The coolant density reactivity

feedback is integrated over the flow channels (Equation (2-20)), and the difference between the initial and transient values (Equation (2-21)) is provided to the Point-Kinetics model for the calculation of fission power.

$$R_{CD}(t) = \sum_{n}^{N} \alpha_c^n \times \rho_c^n(t) \times V_c^n \qquad (2\text{-}20)$$

$$\Delta R_{CD}(t) = R_{CD}(0) - R_{CD}(t) \qquad (2\text{-}21)$$

where $R_{\mathrm{CD}}(t)$ is the integrated coolant reactivity at time t in the unit of Δk/k; α_c^n is the coolant density reactivity coefficient of node n in unit of Δk/k per kg; $\rho_c^n(t)$ is the coolant density of node n at the time of t; V_c^n is the coolant volume of node n; N is the total node number in the flow channel. Together with user-provided coolant density reactivity coefficients, the reactivity feedbacks in response to the coolant temperature changes during the transient impose a positive or negative impact on the fission power.

3 Verification of Thermal Expansion Model

3.1 ABTR Model Description

A typical SFR core model, based on the Advanced Burner Test Reactor (ABTR) conceptual design, has been developed to examine the structure thermal expansion and reactivity feedback modeling capabilities in SAM.

The detailed design parameters of the 250 MW pool type design ABTR can be found in [6]. The primary system is configured in a pool-type arrangement, with the reactor core, primary pumps, intermediate heat exchangers, and direct reactor auxiliary cooling system heat exchangers all immersed in a pool of sodium coolant within the reactor vessel. The reactor core consists of 24 assemblies in an inner enrichment zone and 30 assemblies in the outer zone. A total of nine test locations are provided for fuel (6 assemblies) and material (3 assemblies) tests. On the basis of the reactor physics calculations, a five-channel model was selected to model the reactor core. Channel 1 is used to represent the peak-power inner-core subassembly with fresh fuel. Channels 2 and 4 represent the average subassemblies in the inner and outer enrichment zones respectively, while channel 3 represents the average of the mid-core fuel test assemblies. Channel 5 represents all of the non-fuel subassemblies, including the mid-core materials test assemblies. Figure 3-1 shows the initial subassembly powers at the beginning of equilibrium cycle conditions, and the average axial power shape for all assemblies. The geometric data and input conditions employed in the multi-channel core model are shown in Table 3-1.

Figure 3-2 shows the schematics of the ABTR model to be analyzed with SAM. The primary coolant system consists of the Downcomers (pump outlet and pump discharge), the Inlet Plenum, the Reactor Core Model, the Outlet Plenum, and the intermediate heat exchanger. Five CoreChannels (flow channels with heat structure attached to each of them) were used to describe the reactor core. A Time Dependent Volume component is used to represent the cover gas above the outlet plenum. Different components are connected with Branches. The intermediate loop, the secondary loop, and the DRACS loop are modeled with great simplicities. Single-phase counter current heat exchanger models are implemented to mimic the function of the intermediate loop heat exchanger (IHX), DRACS heat exchanger (DHX), and secondary loop heat exchanger (SHX) to transfer heat among the primary, intermediate, secondary, and the DRACS loops. The geometric data of the non-core components employed in the ABTR model are shown in Table 3-2 and Table 3-3.

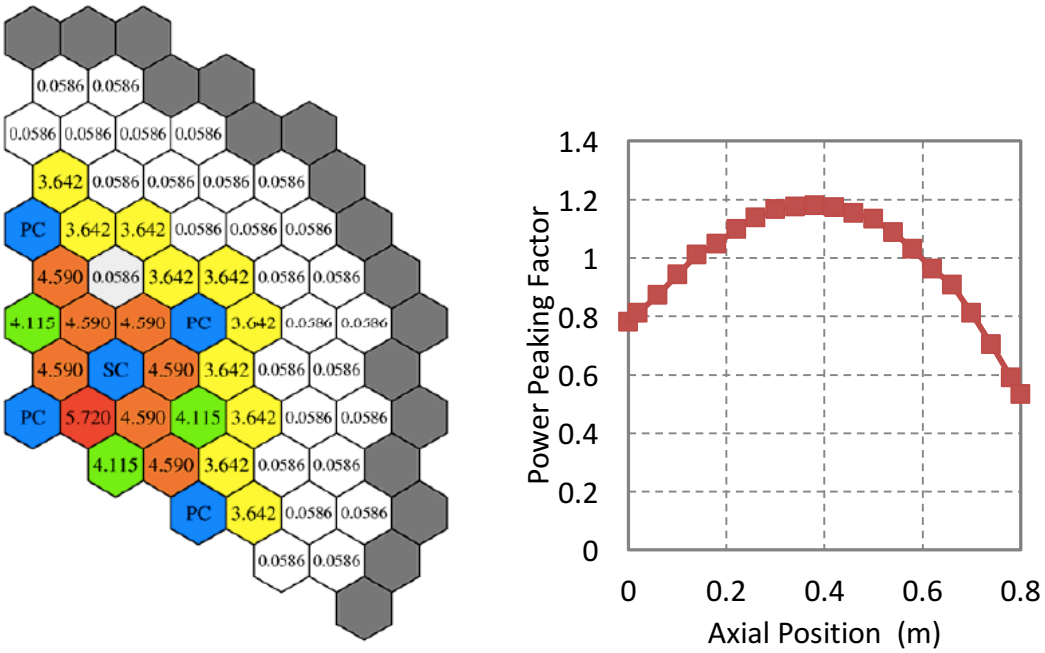

Figure 3-1. Assembly radial (left) [6] and axial (right) power distribution at BOC

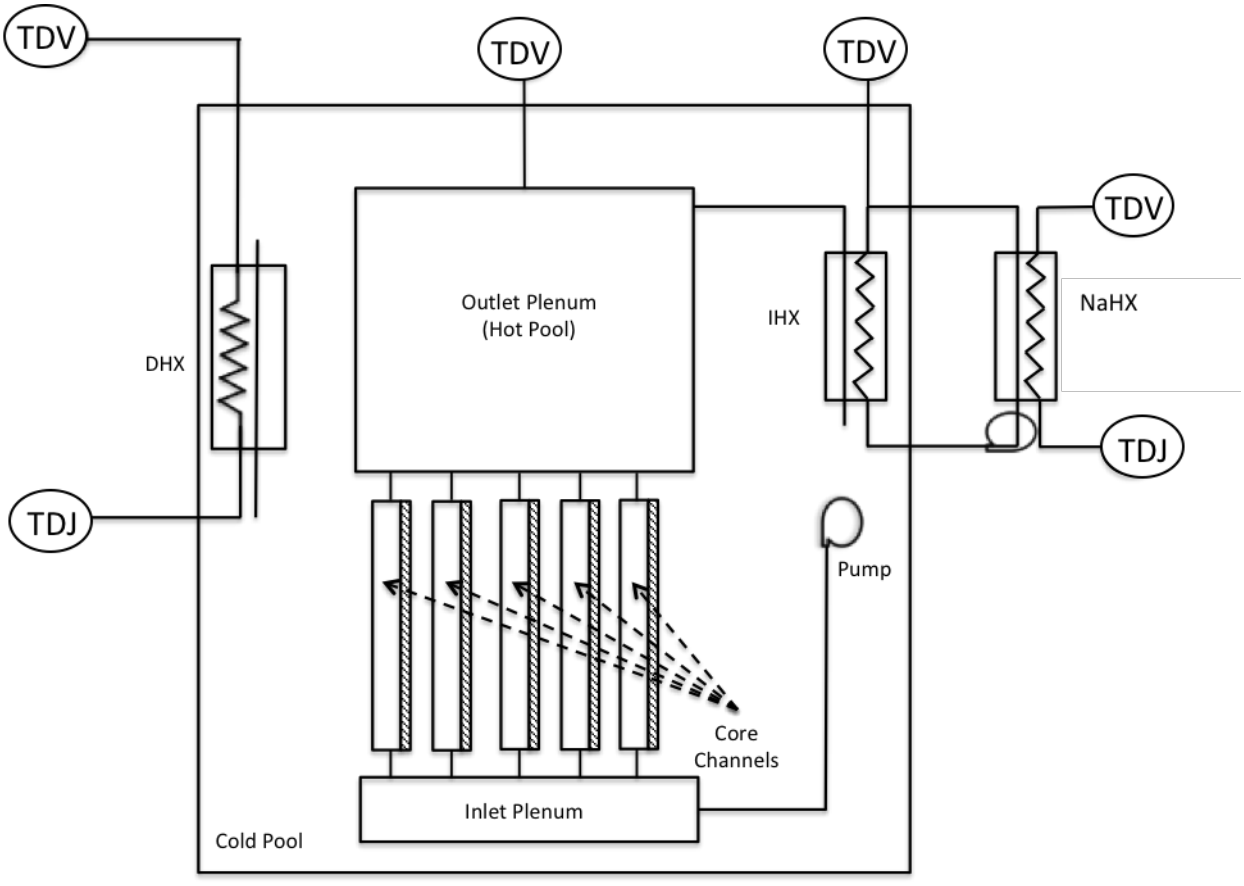

Figure 3-2. Schematics of the test ABTR model

Table 3-1. Coolant channel model data

	Channel 1	Channel 2	Channel 3	Channel 4	Channel 5
Channel Location	Inner Hot Assembly	Inner Core	Fuel Test	Outer Core	Reflector Channel
Assembly number	1	23	6	30	81
Pin number per assembly	217	217	217	217	91
Power per assembly (MW)	5.62	4.56	4.105	3.59	0.0883
Flow Area (m^2)	0.00492	0.113	0.0295	0.148	0.154
Hydraulic Diameter (mm)	2.972	2.972	2.972	2.972	1.694
Channel Height (m)	0.8	0.8	0.8	0.8	0.8
Fuel pellet radius (mm)	3.48	3.48	3.48	3.48	6.32
Cladding thickness (mm)	0.52	0.52	0.52	0.52	0.70
Inlet Orifice Coefficient	0.5	5.15	5.76	13.2	11100

Table 3-2. Geometric input data for major out-of-core 1-D components

Component	Component Type	Inlet Elevation (m)	Flow Area (m^2)	Hydraulic Diameter (m)	Length (m)
Lower Unheated Core	PBPipe	-0.6	*	*	0.6
Active Core	PBCoreChannel	0	*	*	0.8
Upper Unheated Core	PBPipe	0.8	*	*	1.5
IHX Primary Side	PBHeatExchanger	5.88	0.766	0.0186	3.71
IHX Secondary Side	PBHeatExchanger	2.17	0.517	0.014	3.71
Pump Pipe	PBOneDFluid-Component	3.61	0.132	0.34	4.38
Pump Discharge	PBOneDFluid-Component	-0.77	5.36	1	1.26
SHX Primary Side	PBHeatExchanger	5.88	0.766	0.0186	3.71
SHX Secondary Side	PBHeatExchanger	2.17	0.517	0.014	3.71
DHX Primary Side	PBHeatExchanger	6.04	0.024	0.037	2.35
DHX Secondary Side	PBHeatExchanger	3.69	0.024	0.037	2.35

*: channel dependent, see [6]

Table 3-3. Geometric input data for 0-D volume

Component	Type	Geometric Center (m)	Flow Area (m^2)	Total Volume (m^3)	Ref. Liquid Level (m)
Inlet Plenum	PBVolumeBranch	-0.77	4.4934	3.06	-
Outlet Plenum	PBLiquidVolume	6.45	11.16	92.51	3.59
Cold Pool	PBLiquidVolume	2.3	12.8	181.11	4.15

3.2 Coupling scheme

The coupling between SAM and the external thermomechanics modules would be necessary, as it provides the option to accurately calculate the thermal expansion of different components (e.g. grid plate and fuel pin). This capability is developed to provide more accurate predictions of the fuel axial expansion and core radial expansion in Equation (2-4) and Equation (2-14), respectively. The coupling of SAM and the thermomechanics module is achieved through MOOSE's MultiApp mechanism (Figure 3-3). The Tensor Mechanics module from MOOSE is currently coupled with SAM for the calculation of thermal expansion in fuel pin and reactor constraint system.

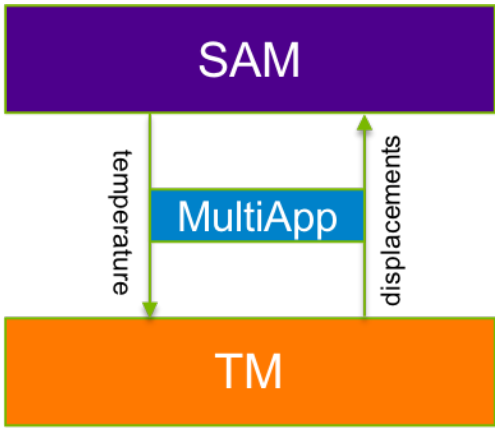

Figure 3-3. Schematic of coupling of SAM and Thermomechanics (TM) module

3.2.1 Overview of MOOSE's Tensor Mechanics Module

The MOOSE Tensor Mechanics module is a library for simplifying the implementation of simulation tools that solve mechanics problems [2]. The strong form of governing equation for the Tensor Mechanics module can be stated as follows:

$$\begin{aligned} \nabla \cdot (\boldsymbol{\sigma} + \boldsymbol{\sigma}_0) + \boldsymbol{b} &= \mathbf{0}\ in\ \Omega \\ \boldsymbol{u} &= \boldsymbol{g}\ in\ \Gamma_g \\ \boldsymbol{\sigma} \cdot \boldsymbol{n} &= \boldsymbol{i}\ in\ \Gamma_i \end{aligned} \qquad (3\text{-}1)$$

where Ω is the domain, $\boldsymbol{\sigma}$ is the Cauchy stress tensor, $\boldsymbol{\sigma_0}$ is an additional source of stress (such as the thermal stress), $\mathbf{u}$ is the displacement vector, $\mathbf{b}$ is the body force, $\mathbf{n}$ is the unit normal to the boundary, $\mathbf{g}$ is the prescribed displacement on the boundary (Γ_g), and $\mathbf{i}$ is the prescribed traction

on the boundary (Γ_i). In the current coupling scheme, the Tensor Mechanics module library is linked with SAM and is thus directly available to SAM.

3.2.2 Coupling Scheme

The coupling scheme for fuel axial expansion is shown in Figure 3-4. In SAM, the heat structure in the core channel component is modeled with an axisymmetric 2D mesh in a cylindrical coordinate. The same mesh is also used in the Tensor Mechanics module, where the displacement fields are calculated in an axisymmetric 2D mesh too. At the beginning of each time step, the solid temperature of SAM's heat structure is transferred to the Tensor Mechanics module. The axial displacement field is then transferred from Tensor Mechanics module to SAM for the reactivity calculation. The axial displacements of heat structures in different core channels are calculated by different Tensor Mechanics simulations.

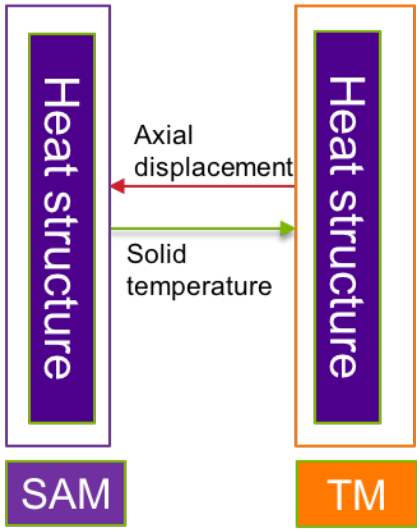

Figure 3-4. Schematic of coupling scheme for fuel axial expansion

The coupling scheme for core radial expansion is shown in Figure 3-5. The core constraint systems are simplified as two grid plates in the lower and upper region of the reactor core. The temperature in the gird plates is assumed to be equal to the coolant temperature at the same elevation. At the beginning of each time step, the inlet/outlet temperature of the core channel are transferred to Tensor Mechanics module for displacement calculation. The grid plates at different locations are modeled separately. Upon finishing the displacement calculation, the relative change in the core radius at different locations are then transferred to SAM for reactivity calculation.

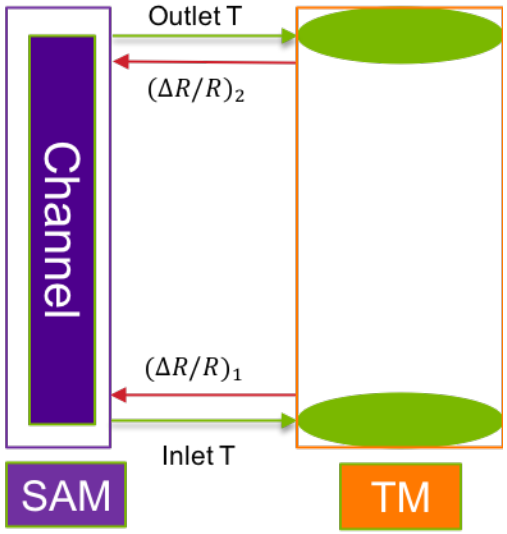

Figure 3-5. Schematic of coupling scheme for core radial expansion

3.3 Verification of Thermal Expansion Model in Fuel Pin

3.3.1 Model Description

An ABTR fuel pin is used to verify the thermal expansion model. The fuel pin is modeled as an axisymmetric 2D mesh in a cylindrical coordinate. The gap between the fuel rod and cladding region is ignored in this test. The geometry parameters and material properties are given in Table 3-4. Two separate tests are performed for the free expansion and eutectic condition expansion, respectively.

Table 3-4. Geometry and material properties of fuel pin

Parameter	Fuel rod region	Cladding region
Outer radius (R)	0.348 cm	0.4 cm
Length (L)	0.8 m	0.8 m
Thermal expansion coefficient (α)	1.76×10^{-5}	1.40×10^{-5}
Stress free temperature (T_{ref})	293.15 K	293.15 K
Thermal conductivity (k)	18.15 W/m K	26.308 W/m K
Young's modulus (E)	28.0 GPa	150.0 GPa
Poisson's ratio (ν)	0.3	0.3

3.3.2 Verification Results

Free expansion. This is a steady-state simulation for verification of the thermal expansion model in the fuel rod under free expansion assumption. For this verification test, the heating power

is assumed to be uniform in the fuel rod, i.e. $q''' = 8.5\times10^8$ W/m^3; the fluid temperature increases linearly from the inlet to the outlet, i.e. $T_{fluid} = 628.15 + 100.0\times z$ K; the heat transfer coefficient is assumed to be constant in the axial direction, i.e. $h = 10^5$ W/m^{2}K. Since this is a steady-state simulation, the analytical temperature in the fuel pin is obtained and then used in Equation (2-10) for calculating the axial displacement in the fuel rod. The comparison of the simulation result and the model prediction is shown in Figure 3-6 for the axial displacements at various locations. The simulation results match the model prediction very well, with a mean relative difference about 0.13%. The small difference may be due to numerical errors and the approximations used in the model such as neglecting the axial thermal conduction.

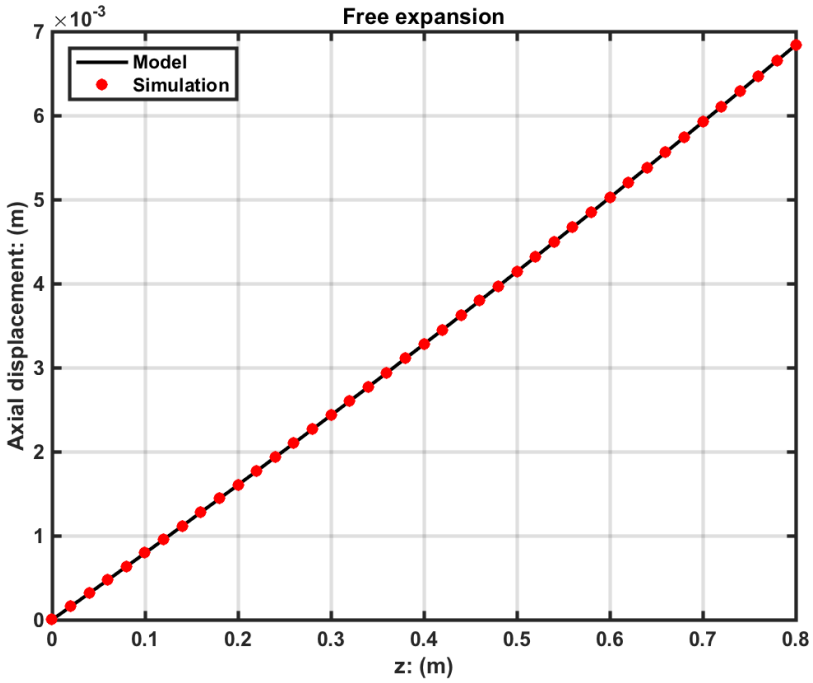

Figure 3-6. Axial displacement in fuel rod under free expansion

Eutectic condition. This is a steady-state simulation for verification of the thermal expansion model in the fuel rod under eutectic condition assumption. For this verification test case, the same heating and inlet conditions are used for the core channel. At steady-state, the temperature in the fuel pin is obtained analytically, which is then used in Equation (2-12) to calculate the axial displacements in the fuel rod and cladding region. The comparison of the simulation result and the model prediction is shown in Figure 3-7. The simulation results match the analytical prediction very well, with a mean relative difference about 0.19%.

Compared with the free expansion case, the axial displacement in the fuel pin is lower in eutectic condition, because the thermal expansion in the cladding is lower than the thermal expansion in the fuel rod, the strong shear force in the rod-cladding boundary reduces the effective axial displacement in the fuel rod.

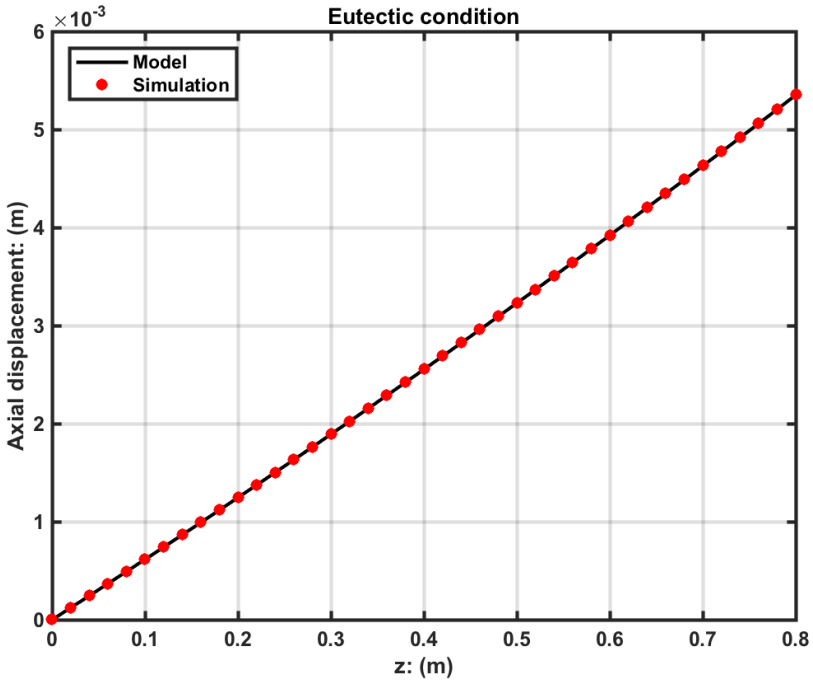

Figure 3-7. Axial displacement in fuel pin under eutectic condition

3.4 Verification of Radial Expansion Model in Grid Plate

3.4.1 Model Description

The ABTR grid plate design is used to demonstrate the radial thermal expansion model in the grid plate. Figure 3-8 shows the geometry for modeling the thermal expansion in the grid plate. There are in total 73 fuel assemblies in the core region. The equivalent core outer diameter is $D_o = 1.31$ m, which is increased to $D_o = 1.5$ m in the simulation model to hold all 73 assemblies in a circular disk. The geometry parameters and material properties are given in Table 3-5.

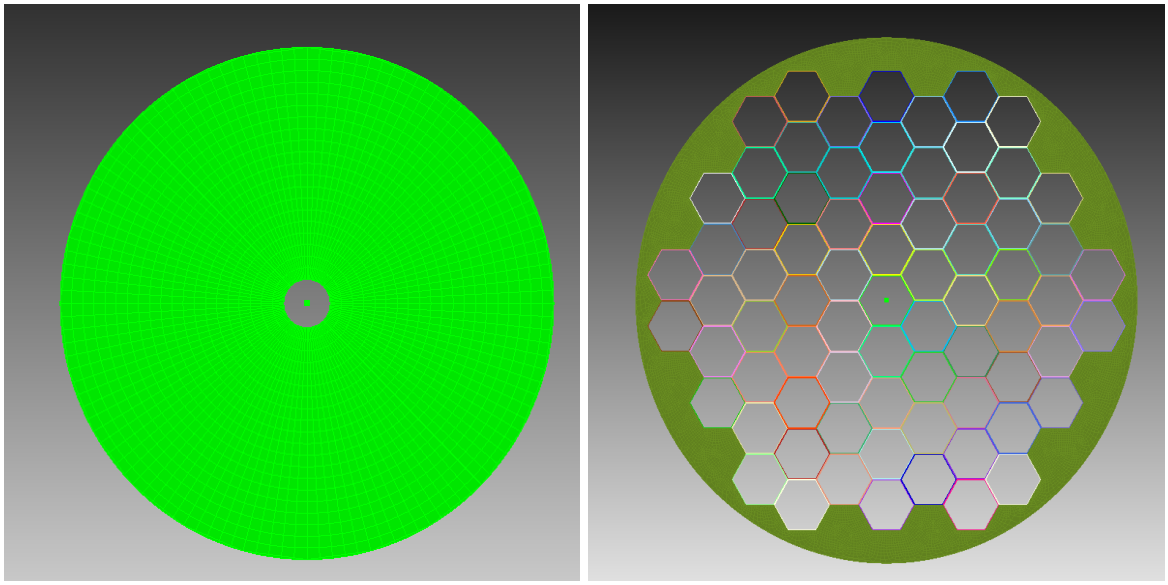

Figure 3-8. Mesh for a hollow disk (left) and a grid plate (right)

Table 3-5. Geometry and material properties of grid plate

Parameters	Values
Outer radius (R_o)	0.75 m
Assembly pitch (P)	14.598 cm
Gap width (G)	0.4 cm
Thermal expansion coefficient (α)	1.60×10^{-5}
Stress free temperature (T_{ref})	293.15 K
Thermal conductivity (k)	15.0 W/m K
Young's modulus (E)	200.0 GPa
Poisson's ratio (ν)	0.3

3.4.2 Verification Results

For this verification test, a uniform temperature, $T = 638.15$ K, is applied to the grid plate. The comparison of simulation results and the model prediction is shown in Figure 3-9. It is seen that the simulation results match the prediction very well with a mean relative difference much smaller than 0.1%. Note that there is no significant difference in the radial displacement in the hollow disk and in the grid plate, thus it is reasonable to simplify the grid plate as a hollow disk for the fast simulation model.

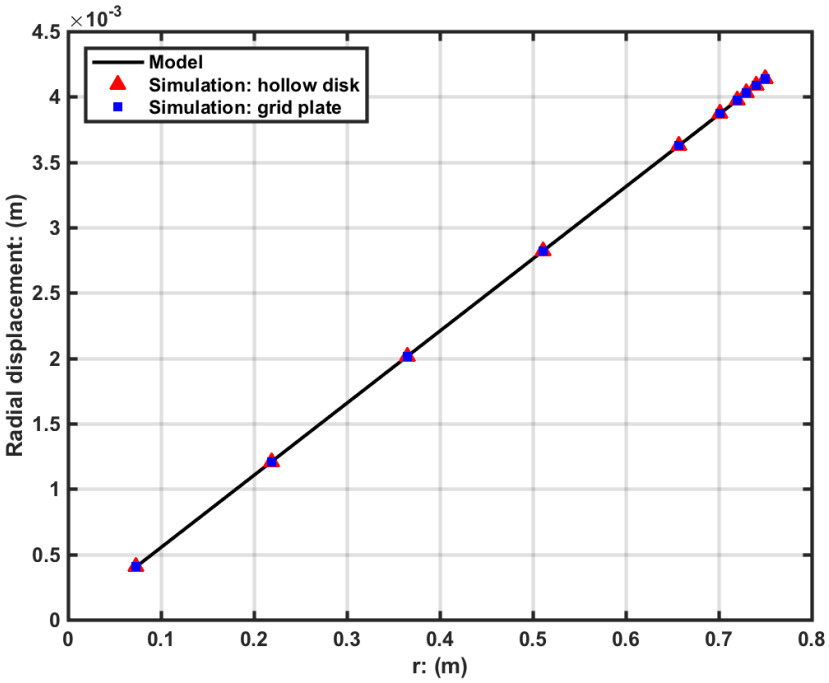

Figure 3-9. Verification of thermal expansion in grid plate

4 Demonstration of Reactivity Feedback Mechanisms

The heat transport system of the ABTR preconceptual design is used to demonstrate the point kinetics and reactivity feedback modeling capabilities in SAM. The model for the ABTR heat transport system was discussed in Section 3.1. The major components in the ABTR heat transport system are reactor core, inlet/outlet plenum, cold/hot pool, pump, direct reactor auxiliary cooling system (DRACS), and intermediate heat transfer system (IHTS). In SAM model, the reactor core is modeled with 5 core channels (CH1 to CH5), the DRACS is modeled with one heat exchanger (DHX), and IHTS is modeled with two heat exchangers (IHX and NaHX).

4.1 Demonstration of Separate Reactivity Feedback

4.1.1 Model Description

A test case simplified from the ABTR model is used to demonstrate the individual reactivity feedback model. The test case is based on a single channel model with increasing inlet coolant temperature from 628.15K to 728.15K in the 100s of the transient. The initial fission power is 3×10^4 W and the initial flow rate is 0.147 kg/s. The transient starts from a steady-state status corresponding to the given initial fission power and initial flow rate. Four separate reactivity test cases are used to test the individual reactivity feedback model, i.e. only the reactivity model being tested was activated in the test case.

4.1.2 Verifications of Separate Reactivity Feedback Modeling

Axial expansion reactivity feedback. For this test, the geometry parameters and material properties of the fuel pin are given in Table 3-4. The fuel and the cladding are assumed in eutectic condition. The input fuel reactivity coefficient (i.e. r_f in Equation (2-4)) is given by Equation *(4-1)*.

$$r_f(z) = \begin{cases} 10^{-4}\ (z < 0) \\ 1.2\times10^{-4}(0 \le z < 0.1) \\ 1.3\times10^{-4}\ (0.1 \le z < 0.3) \\ 1.2\times10^{-4}(0.3 \le z < 0.4) \\ 10^{-4}(z \ge 0.4) \end{cases} \qquad (4\text{-}1)$$

Figure 4-1 shows the transient fuel axial expansion reactivity given by SAM standalone simulation and SAM-TM coupled simulation. The fuel axial expansion reactivity from SAM standalone simulation matches well with that from the SAM-TM coupled simulation. The coupling scheme is working as expected. The average temperature in the fuel pin increases as the inlet coolant temperature increases during the transient, which brings in the negative reactivity feedback. But the magnitude of the negative reactivity is almost negligible, the reactor power reduces slowly. With the conditions that the inlet coolant temperature increases linearly during the transient and the reactor power reduces slowly, the mean temperature in the fuel pin increases roughly linearly with time, which gives the linearly decreasing fuel axial expansion reactivity, as is shown in Figure 4-1.

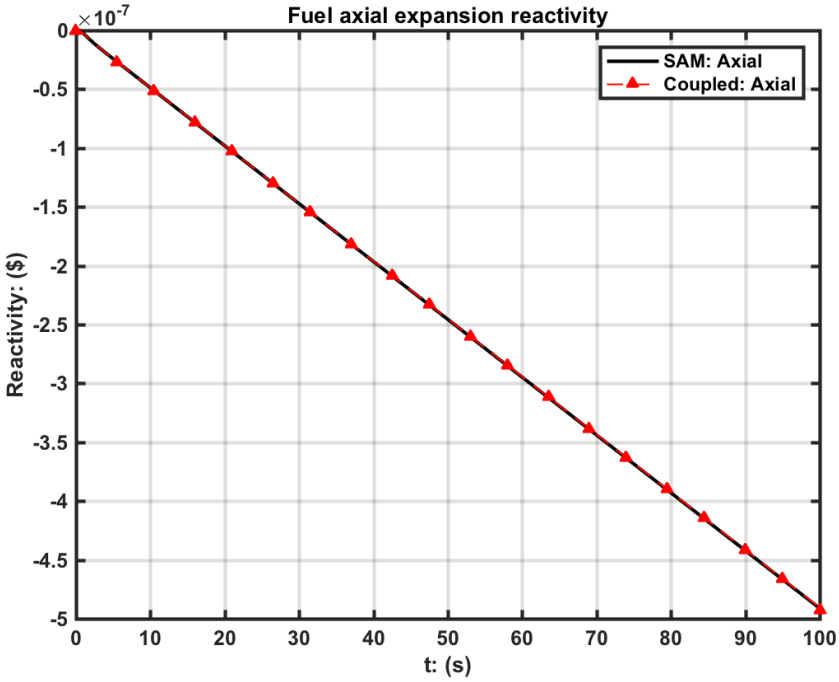

Figure 4-1. Single-channel transient fuel axial reactivity.

Core radial expansion feedback. For this test, the geometry parameters and material properties of the grid plate are given in Table 3-5. The input core radial expansion reactivity coefficients (i.e. $\rho_{\mathrm{RC},n}$ in Equation (2-14)) are -0.4625 for both the lower and upper grid plate positions; but the weighting factors (i.e. w_n in Equation (2-14)) are 0.75 and 0.25 for the lower and upper positions, respectively. Note that the weighting factors are set randomly for test purposes. Figure 4-2 shows the transient core radial expansion reactivity given by SAM standalone simulation and SAM-TM coupled simulation. The core radial expansion reactivity from SAM standalone simulation matches well with that from the SAM-TM coupled simulation. The coupling scheme is working as expected. The temperatures in the lower and upper grid plate are assumed to be equal to the coolant temperature at the inlet and outlet of the channel, as is shown in Figure 4-3. The inlet coolant temperature increases during the transient, which causes the increase in the outlet coolant temperature at the beginning of the transient when the reactor power is still large. The radial expansion in both the lower and upper part brings in the negative reactivity feedback, which in turn brings down the reactor power and the outlet coolant temperature. The transient profile of the total reactivity is a combination of the transient profile of the inlet coolant temperature (increases linearly with time) and the outlet coolant temperature (increases in the beginning but decreases near the end of the transient). Since the weighting factor of the lower part (0.75) is larger than that of the upper part (0.25), the total reactivity is roughly following the transient profile of the inlet coolant temperature.

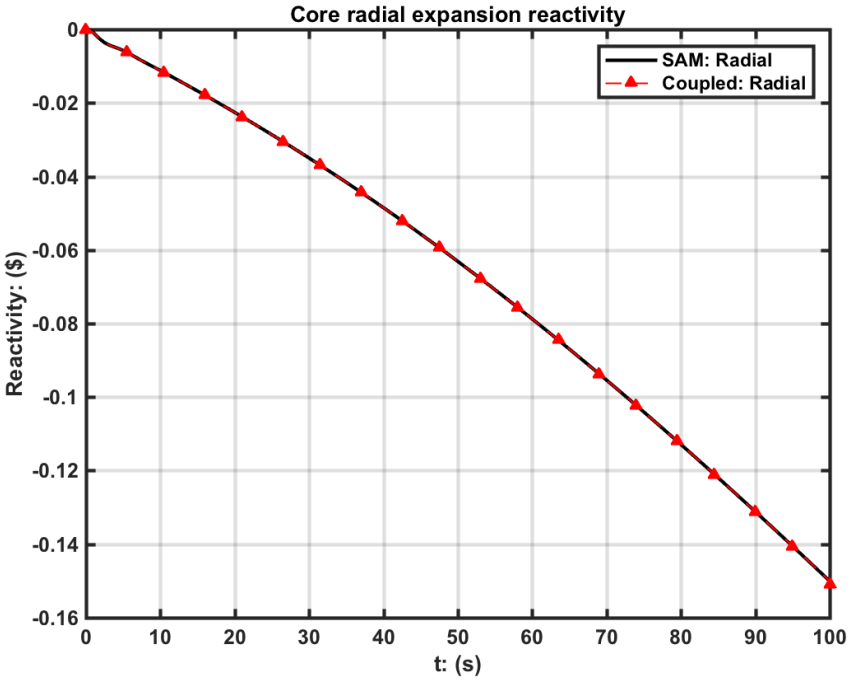

Figure 4-2. Single-channel transient core radial expansion reactivity.

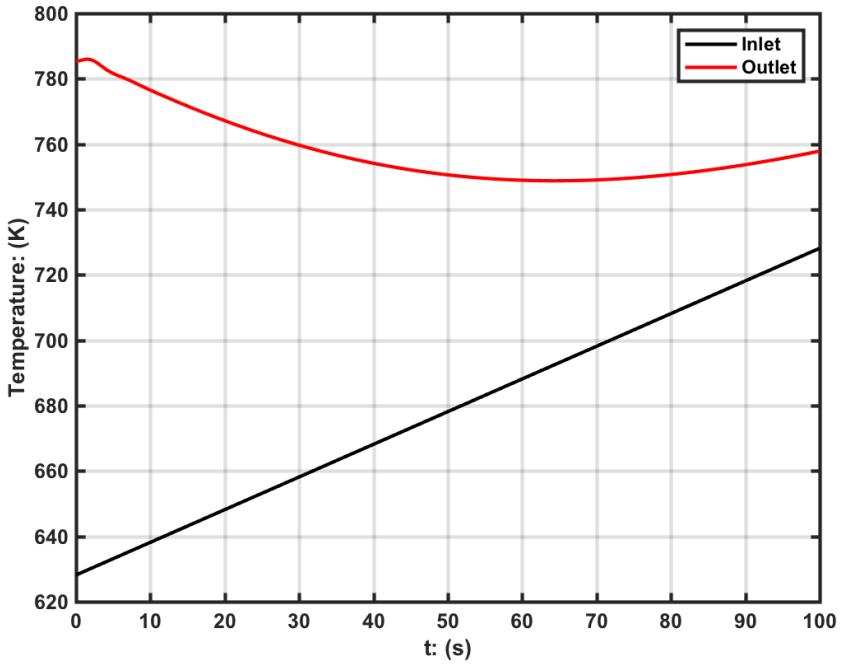

Figure 4-3. Transient coolant temperature at the inlet and outlet of the channel

Fuel Doppler reactivity feedback. The input fuel Doppler reactivity coefficient (i.e. α_D^n in Equation (2-19)) is -1.2878×10^{-7} for this test. In this test, the fuel Doppler reactivity coefficient

is set to be very small that the reactor power does not change much during the transient and a reference value for the reactivity can be obtained analytically. The inlet coolant temperature increases during the transient, which causes the increase in the fuel temperature. The increasing fuel temperature brings in negative reactivity to the reactor. There is a total of 0.39% decrease in the reactor power at the end of the transient. In this test, a reference value for the fuel Doppler reactivity could be obtained with

$$R_D^{ref}(t) \approx -1.2878\times10^{-7}\sum_{n}^{N} ln\left[\frac{T_f^n(0)+100\times t}{T_f^n(0)}\right] \qquad (4\text{-}2)$$

where $T_f(0)$ is the average fuel temperature at the steady-state, which is shown in Figure 4-4. Figure 4-5 shows the comparison of the transient fuel Doppler reactivity given by SAM and the reference value given by Equation (4-2). The simulation result matches the reference value very well.

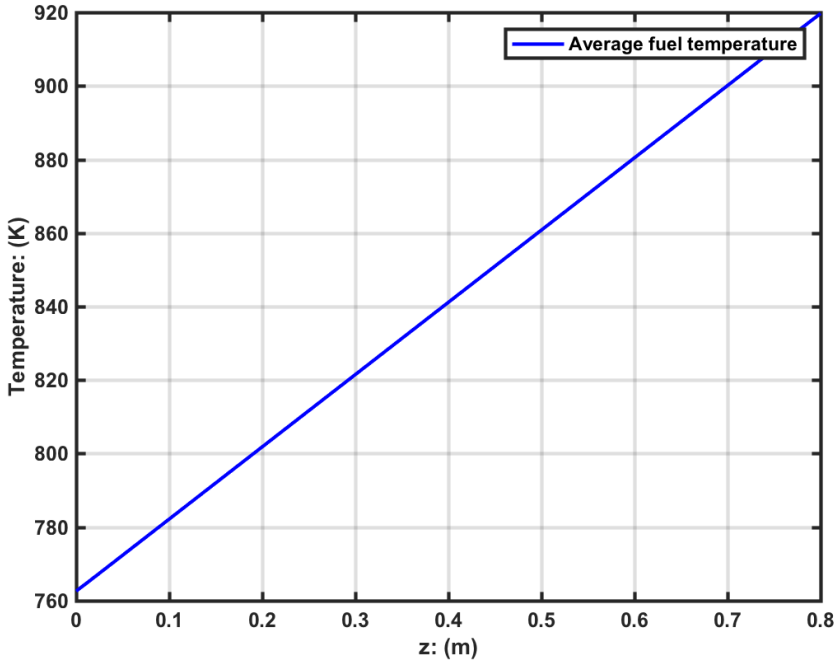

Figure 4-4. Single-channel average fuel temperature at the beginning of the transient.

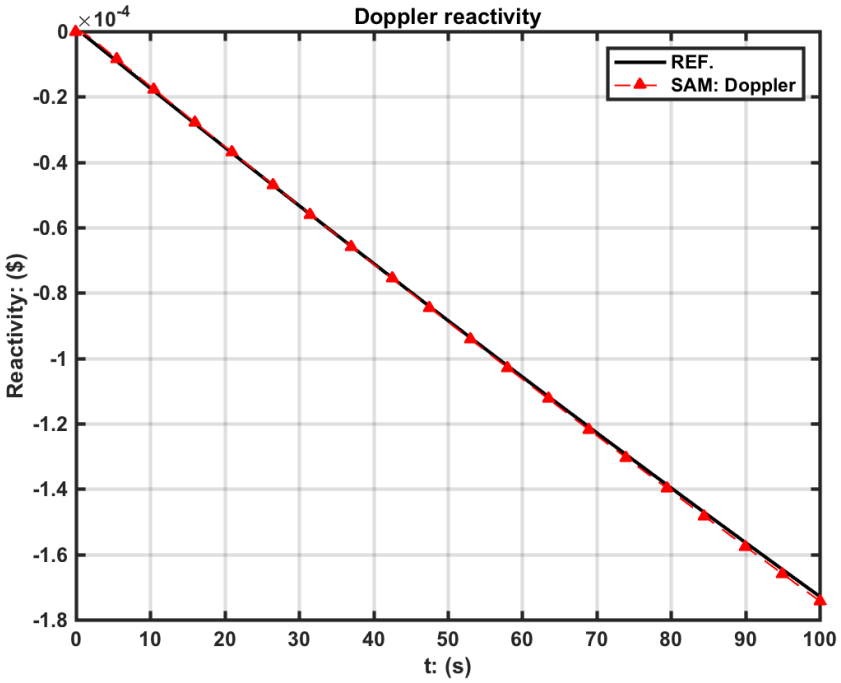

Figure 4-5. Single-channel transient fuel Doppler reactivity.

Coolant density reactivity feedback. The coolant density reactivity coefficient (i.e. α_c^n in Equation (2-20)) is 1.0×10^{-3} for this test. In this test, the coolant density reactivity coefficient is also set to be a small value that the reactor power changes slowly during the transient and a reference value for the reactivity can be obtained analytically. The inlet coolant temperature increases during the transient, which causes the decrease of the coolant density in the channel. The decreasing coolant density brings in positive reactivity to the fast reactors. There is a total of 0.26% increase in the reactor power at the end of the transient. In this case, a reference value for the coolant density reactivity could be obtained with

$$\Delta R_{CD}^{ref}(t) \approx \sum_{n}^{N} \alpha_c^n \times \frac{\partial \rho_c}{\partial T_c} \times (100\times t) \times V_c^n \qquad (4\text{-}3)$$

where $\frac{\partial \rho_c}{\partial T_c} = -0.2382\ \mathrm{kg/m^3K}$ is a constant value during the transient. Figure 4-6 shows the comparison of the transient coolant density reactivity given by SAM and the reference value given by Equation (4-3). The simulation result matches the reference value well. The difference is caused by the assumptions used in the reference model that power is unchanged, and that density is a linear function of temperature.

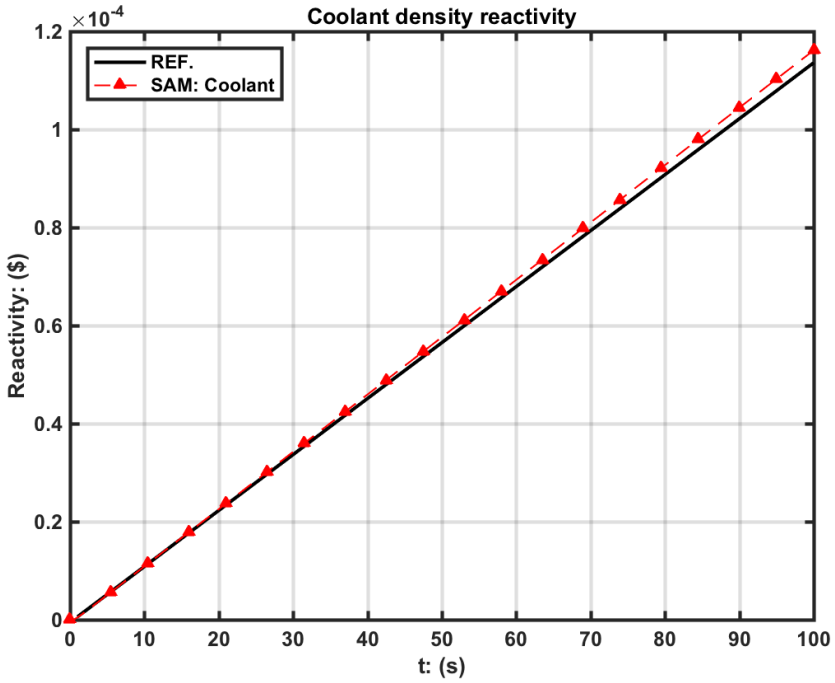

Figure 4-6. Single-channel transient coolant density reactivity.

The demonstration results for the four separate reactivity models show that the individual reactivity feedback model is implemented correctly in SAM. The fuel axial expansion reactivity and core radial expansion reactivity given by the coupling scheme match the corresponding reactivity given by SAM standalone simulation. The reactivity feedback models and the coupling scheme are working as expected and are ready for a more complex demonstration test, e.g. an unprotected loss-of-flow (ULOF) accident.

4.2 Demonstration of Unprotected Loss-of-flow (ULOF) Accident

4.2.1 Model Description

The ABTR model described in Section 3.1 is used in the test. An unprotected loss-of-flow (ULOF) accident is selected as the demonstration case. As described in Section 3.1, Channel 2, 3, and 4 represent the majority of the fuel assemblies in the reactor core, thus these channels are used the calculate the fuel axial expansion. The input fuel reactivity coefficients for each individual channel are different and are shown in Figure 4-7. The fuel and the cladding are assumed in eutectic condition in this test. The input core radial expansion reactivity coefficients are -0.86929 for both the lower and upper positions; but the weighting factors are 0.3 and 0.7 for the lower and upper positions, respectively. The weighting factor strongly depends on the radial deformation of the core during the actual transient, which is very hard to predict. Thus, these weighting factors are chosen only for demonstration purposes. The input fuel Doppler reactivity coefficients for each individual channel are shown in Figure 4-8. The input coolant density reactivity coefficients for each individual channel are shown in Figure 4-9. The other reactivities, e.g. control rod drive line thermal expansion reactivity, are given as external reactivity in the input file, which is shown in

Figure 4-10. Note that most of the reactivity coefficients are taken from a previous work on ABTR design analysis [6].

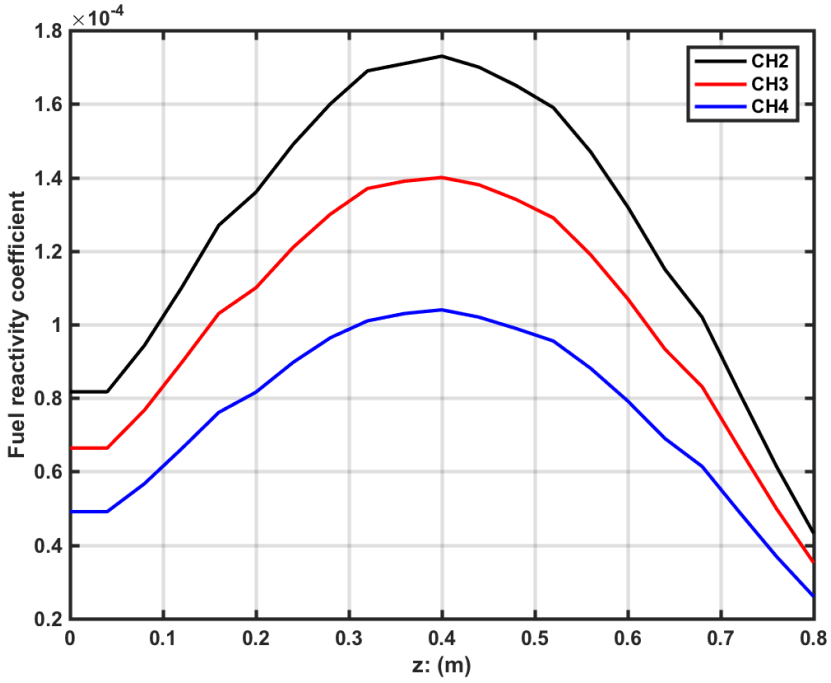

Figure 4-7. Input ABTR fuel axial expansion reactivity coefficient for 3 channels.

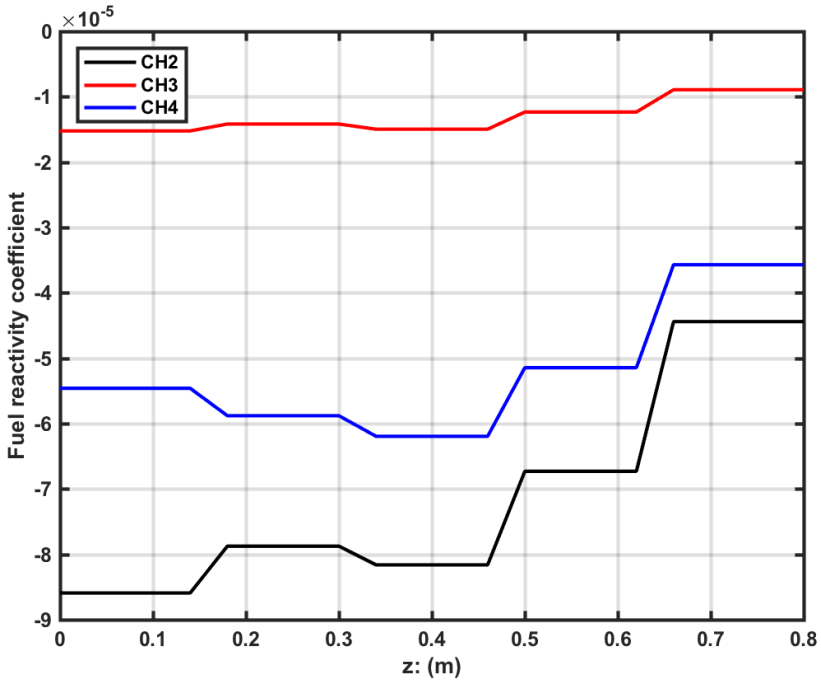

Figure 4-8. Input ABTR fuel Doppler reactivity coefficient for 3 channels.

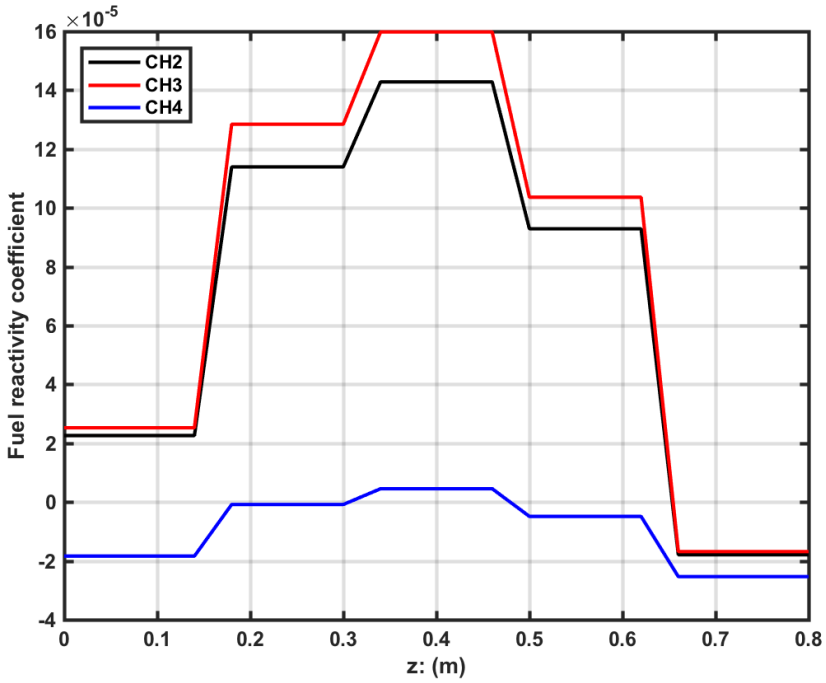

Figure 4-9. Input ABTR coolant density reactivity coefficient for 3 channels.

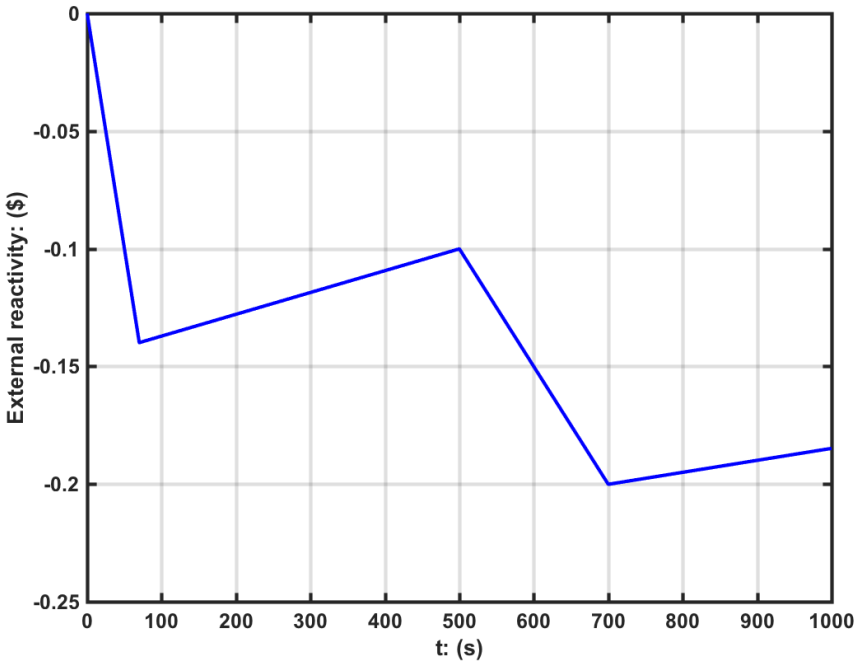

Figure 4-10. Input ABTR transient external reactivity

4.2.2 Accident Sequences

The accident sequence analyzed here is the loss of normal power to the reactor and intermediate loss of forced flow in the primary and intermediate coolant circuits. A programmed flow coast down of the coolant pumps is assumed to operate. The pump coast down curve during the transient is shown in Figure 4-11. In addition, it is assumed that heat removal at the sodium-CO2 heat exchanger ceases, so that the only heat removal path is through the emergency direct reactor auxiliary cooling system (DRACS). The initial condition for the accident sequence is the normal operation at full power and flow. With the loss of pumping power, flow in the primary circuit coasts down according to the programmed pump head decay. The system is running for 500s to reach the normal operation status before the transient simulation starts. Following the pump flow coast down, natural circulation flow is established.

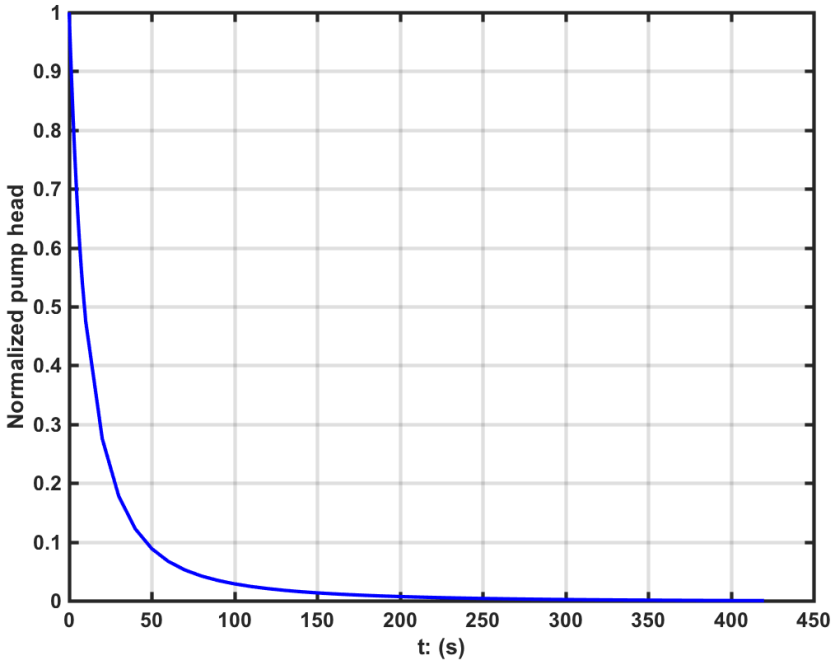

Figure 4-11. ABTR pump coast down transient

There are two variations of the loss-of-flow accident sequence. In the first, the reactor safety system acts to insert control rods and reduce reactor power to decay heat. This sequence is called protected loss-of-flow (PLOF) accident. In the second, the reactor safety system fails to insert the scram control rods and the loss of forced flow proceeds at full power. This sequence is called the unprotected loss-of-flow (ULOF) accident. The ULOF accident is used to demonstrate the Point-Kinetics model and the reactivity feedback models.

In the ULOF accident, the reactor power remains at full power initially and is reduced later due to the inherent negative reactivity feedbacks. As the coolant flow rate decreases, reactor temperatures increase within the first minute. During this time, the peak fuel and cladding temperatures rise. This increase in temperatures provides the driving force for establishing the natural circulation flow, which will then reduce the peak fuel and cladding temperatures. The reactor seeks equilibrium with the available heat sink by reducing power. This will reduce the reactor temperature and establish a quasi-equilibrium condition. However, the reactor system will

continue to heat slowly until the decay heat falls below the heat rejection capacity of DRACS system. When decay heat production falls below the DRACS capacity, the system temperature starts to decline.

4.2.3 SAM Results

Figure 4-12 shows the histories for the total reactor power, the heat removal rate from IHTS (IHX) and DRACS (DHX) heat exchangers, and the coolant flow in the hot channel (CH1). Figure 4-13 shows the transient peak fuel, peak cladding, CH1 coolant outlet, cold pool, and hot pool temperatures. Figure 4-14 shows the transient radial core expansion, axial fuel expansion, coolant density, and Doppler reactivity feedbacks. The coolant and cladding temperatures increase significantly during the first 30 seconds, which contribute to the negative radial and axial reactivities. The negative radial and axial reactivities are the main factors to bring down the reactor power and fuel temperatures. For this demonstration case, the coolant density and Doppler effect bring in the positive reactivities, but in a smaller magnitude. The flow coast-down by the inertia of the primary pumps ends at approximately 450 seconds when the natural circulation has not yet been fully established. Shortly after this point, the peak fuel, peak cladding, and coolant temperatures begin to rise to form a second temperature peak. The increased temperatures become the driving force to increase the natural circulation flow rate.

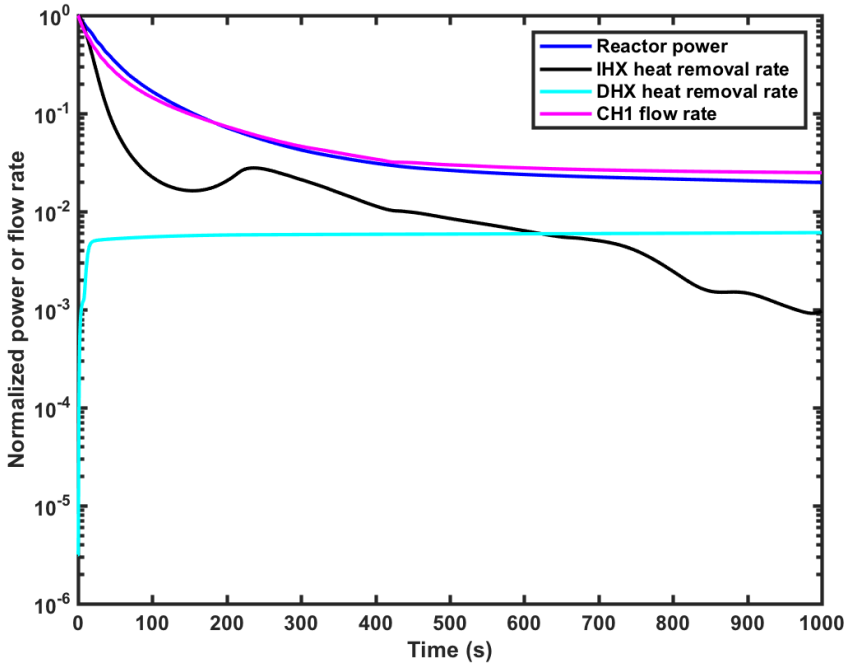

Figure 4-12. ABTR ULOF transient reactor power, heat removal rate, and flow rate

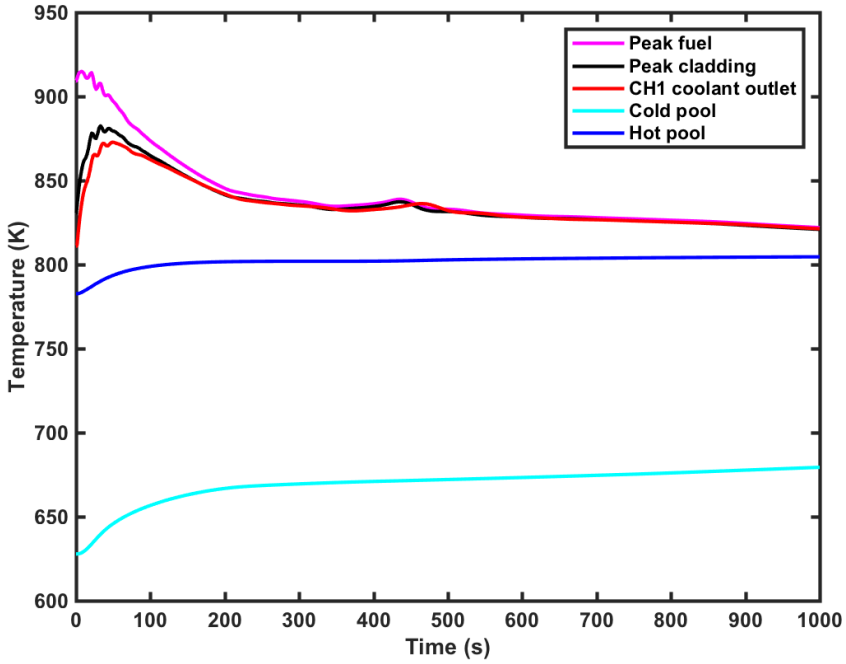

Figure 4-13. ABTR ULOF transient temperatures.

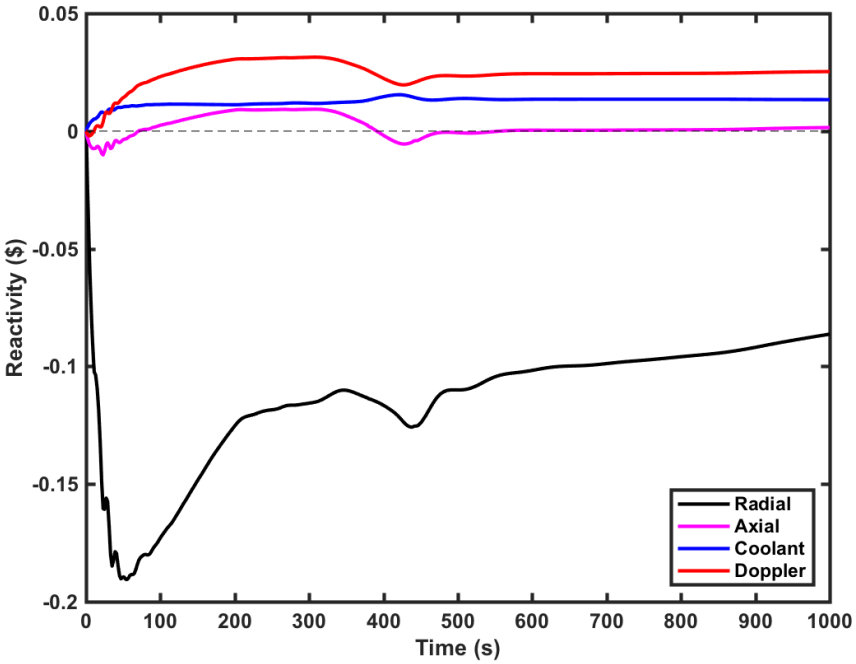

Figure 4-14. ABTR ULOF transient reactivity feedbacks

The radial and axial expansion reactivities from SAM standalone simulation and the coupled SAM and Tensor Mechanics module simulation are compared in Figure 4-15. In SAM standalone simulation, the radial core expansion and axial fuel expansion are calculated internally by SAM;

while in the coupled simulation, the core radial expansion and fuel axial expansion are provided by the Tensor Mechanics module. The reactivities from SAM standalone simulation match well with that from the coupled simulation except for the bias in the fuel axial expansion reactivity. The bias in the reactivity affects significantly the reactor power, which in turns affect the fuel temperature and axial reactivity. The bias comes from the approximations made in the internal models for calculating the axial displacement (Equation (2-10)). Two major approximations are made in Equation (2-10). The first approximation is related to the general plane-strain assumption [7], made in deriving Equation (2-10). The second approximation is the cross-sectional averaged temperature, which is currently approximated with the temperature at a few nodes. Improvement on the fuel axial expansion reactivity feedback model will be implemented later.

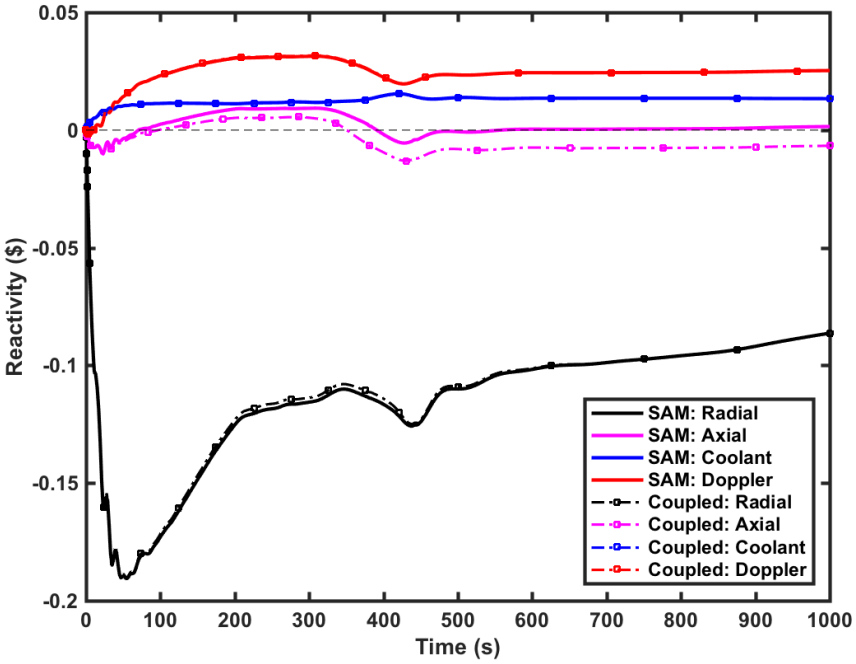

Figure 4-15. ABTR ULOF transient reactivity feedbacks from SAM standalone simulation and coupled simulation

5 Summary

Effort has been put recently to develop, implement, and test the Point-Kinetics module in SAM. Various reactivity feedback models are developed to work with the Point-Kinetics module, including fuel axial expansion, core radial expansion, fuel Doppler, and coolant density reactivity. Extensive verification tests are performed for the Point-Kinetics module and the separate reactivity feedback models.

Simplified thermal expansion models for the fuel pin and reactor constrain system (e.g. grid plate) are developed for the calculation of the reactivity feedback due to thermal expansion of various components. Verification tests for the fuel axial and core radial expansion model are developed. In order to improve the accuracy in predicting the thermal expansion of different components, a coupling interface is developed to enable the coupling of SAM with external thermomechanical analysis modules. Note that the simplified thermal expansion models in SAM are important for fast simulations in reactor safety analysis; while the coupled thermomechanics module provides accurate thermal expansion results for verification purposes.

These new capabilities in SAM are expected to enable simulations under postulated transient scenarios, including loss of flow in the cooling systems and reactivity driven transients. These new capabilities have been demonstrated by simulating the early stage of the ULOF accident in ABTR. It is confirmed that the major physics phenomena in the heat transport system of the ABTR reactor are captured by SAM. The point kinetics models, reactivity feedback models, and the coupling schemes are working well as expected.

Acknowledgement

The authors sincerely thank Mr. Joseph Kelly and Dr. Stephen Bajorek at U.S. Nuclear Regulatory Commission for the fruitful discussions throughout the work and the valuable comments of the report.

This report was prepared as an account of work sponsored by an agency of the U.S. Government. Neither the U.S. Government nor any agency thereof, nor any of their employees, makes any warranty, expressed or implied, or assumes any legal liability or responsibility for any third party's use, or the results of such use, of any information, apparatus, product, or process disclosed in this report, or represents that its use by such third party would not infringe privately owned rights. The views expressed in this paper are not necessarily those of the U.S. Nuclear Regulatory Commission.

Reference:

[1] R. Hu, "SAM Theory Manual", Nuclear Engineering Division, Argonne National Laboratory, ANL/NE-17/4, Argonne, IL, March, 2017.

[2] Gaston, D., Newman, C., Hansen, G., Lebrun-Grandi'E, D., "MOOSE: A Parallel Computational Framework for Coupled Systems of Nonlinear Equations," *Nuclear Engineering and Design*, 239, p. 1768–1778 (2009).

[3] Balay, S., et al, "PETSc Users Manual: Revision 3.10". No. ANL-95/11 Rev 3.10. Argonne National Laboratory (2018).

[4] Fanning, T. H. "The SAS4A/SASSYS-1 Safety analysis code system." *Argonne National Laboratory, ANL/NE-12/4* (2012).

[5] Zhang, G., Hu, R., "Development of MSR Transient Safety Analysis Capability in SAM", *2018 American Nuclear Society Annual Meeting,* Philadelphia PA (2018).

[6] Chang, Y., et. al, "Advanced Burner Test Reactor Preconceptual Design Report", *ANL-ABR-1. Argonne National Laboratory* (2008).

[7] Richard, B. Hetnarski, and M. Reza Eslami. "Thermal stresses-advanced theory and applications." (2008).

Nuclear Science and Engineering Division
Argonne National Laboratory
9700 South Cass Avenue, Bldg. 208
Argonne, IL 60439

www.anl.gov

Argonne National Laboratory is a U.S. Department of Energy laboratory managed by UChicago Argonne, LLC